ISSN (Print) 1226-1750
ISSN (Online) 2233-6656
Journal of Magnetics 24(1), 123-127 (2019) https://doi.org/10.4283/JMAG.2019.24.1.123

The Effect of Mn/Al Substitution on the Structural Stability and Magnetic Properties of Mn_3AlC

Xin-You Wang[1,2], Ping-Zhan Si[1,2]*, Hui-Dong Qian[2], Yang Yang[2], Hong-Liang Ge[1], Jihoon Park[2], Xin-Qing Wang[1], and Chul-Jin Choi[2]*

[1]*College of Materials Science and Engineering, China Jiliang University, Hangzhou 310018, China*
[2]*Powders and Ceramics Division, Korea Institute of Materials Science, Changwon 51508, Republic of Korea*

(Received 23 June 2018, Received in final form 18 December 2018, Accepted 28 February 2019)

The structural stability and magnetic properties of $Mn_{3+x}Al_{1-x}C$ antiperovskite with varied Mn/Al substitution were studied systematically. Single phase $Mn_{3+x}Al_{1-x}C$ alloys with antiperovskite structure were obtained in samples with x = –1/4, 0, 1/4, 1/2. An additional $Mn_{23}C_6$ phase was precipitated from $Mn_{3+x}Al_{1-x}C$ antiperovskite for x = 3/4 while $Mn_{23}C_6$ phase was formed as major phase for x = 1. The mutual substitution of Mn and Al atoms has substantial effect on the Curie temperature and the saturation magnetization of the $Mn_{3+x}Al_{1-x}C$ alloys. In comparison with the as-cast alloys, the as-annealed $Mn_{3+x}Al_{1-x}C$ alloys exhibit reduced Mn/Al substitutions after high temperature homogenization, which enhances the ordering of Mn and Al atoms in the lattices. The Curie temperature of the homogenized $Mn_{3+x}Al_{1-x}C$ increases with increasing Mn substitution to Al. The Mn_3AlC alloy shows the highest saturation magnetization among all samples with varied Mn/Al ratios. Most samples show zero coercivity and zero remanent magnetization. The maximum value of the magnetic entropy changes of $Mn_{2.75}Al_{1.25}C$ at 285 K is 2.26 J/kg K in fields up to 3 T.

Keywords : Mn_3AlC, Mn_4C, magnetic properties, substitution, magnetocaloric effect

1. Introduction

The antiperovskite compound Mn_3AlC, in which the Mn atoms are located at the face-centered position, the Al atom at the cubic corners and the C atom at the body centered position, as shown in Fig. 1, has been studied systematically for more than 5 decades [1]. The research interests of the previous work were mainly focused on the structure, magnetic properties, elastic properties, transport behaviors, and magnetocaloric effect of single phase Mn_3AlC [1-5]. In fact, the single-phase ternary alloys of Mn, Al, C with face-centered-cubic (fcc) structure may present over a wide range of composition with varied Mn/Al substitutions. The varying local environments of Mn atoms with varying Mn/Al ratio and carbon stoichiometry may reflect different physical properties of $Mn_{3+x}Al_{1-x}C_y$. The influence of carbon content on the structural, magnetic and transport properties of Mn_3AlC_x has been studied [6]. However, the reports on the Mn-Al-C ternary system with compositions other than stoichiometric Mn_3AlC are limited. In this work, the $Mn_{3+x}Al_{1-x}C$ alloys with varied x values were prepared and their magnetic properties were studied systematically.

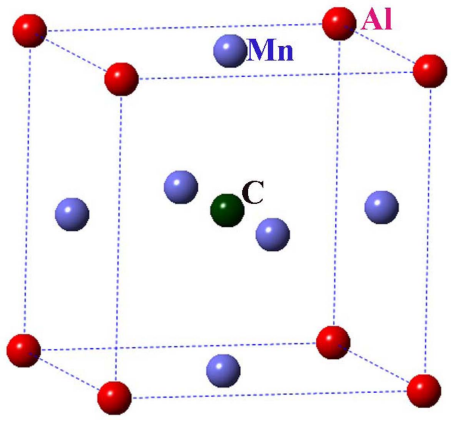

Fig. 1. (Color online) The crystal structure of Mn_3AlC, in which the Mn atoms are located at the face-centered positions, the Al atom at the cube corner and the C atoms at the body-centered position.

*Co-corresponding author: Tel: +86-13221019908
e-mail: pzsi@cjlu.edu.cn, cjchoi@kims.re.kr

This paper was presented at the IcAUMS2018, Jeju, Korea, June 3-7, 2018.

A full substitution of Al with Mn, i.e. Mn_4C, in $Mn_{3+x}Al_{1-x}C$ had long been thought to be impossible for Mn_4C is unstable [7]. Our recent work showed that the metastable Mn_4C may also present at room temperature, even though Mn_4C tends to decompose into $Mn_{23}C_6$ at elevated temperatures [8]. It is known that the $Mn_{3+x}Al_{1-x}C$ become thermally unstable when x is approaching 1 at high temperatures, but the exact composition range is unknown. This work covers the composition range of $Mn_{3+x}Al_{1-x}C$ with x from −1/4 to 1. The Mn/Al ratio in $Mn_{3+x}Al_{1-x}C$ was found to have substantial effects on the structural stability and magnetic properties of this compound.

2. Experimental

The $Mn_{3+x}Al_{1-x}C$ alloys with nominal composition of x = −1/4, 0, 1/4, 1/2, 3/4, and 1 were prepared by induction melting the mixture of high purity Mn flakes, Al granules and graphite powders. The as-cast samples were sealed in an evacuated quartz tube and then homogenized at 1273 K for 24 hours. The structure of the samples was recorded at room temperature by using a Rigaku A/Max 2500 automatic X-ray diffractometer (XRD) operating at 40 kV with Cu-$K\alpha$ radiation. The magnetic properties of the samples were measured by using a Quantum Design physical property measurement system in magnetic fields up to 3 T and at temperatures from 5 K to 930 K. The temperature dependence of magnetization of the homogenized samples under an applied field of 3 T was measured with an increasing temperature rate of 20 K/min.

3. Results and Discussion

Figure 2 shows the XRD patterns of the samples measured at room temperature. The XRD patterns of the as-cast $Mn_{3+x}Al_{1-x}C$ (x = −1/4, 0, 1/4, 1/2 and 3/4) alloys could be indexed with cubic perovskite-type structure, as shown in Fig. 2(a). The crystal structure of Mn_3AlC depicted in Fig. 1 belongs to space group $Pm\bar{3}m$ (Strukturbericht $L'l_2$) with a = 3.87 Å. However, a considerable amount of $Mn_{23}C_6$ and trace amount of Mn were detected in $Mn_{3.75}Al_{0.25}C$, indicating unstable characteristics of fcc $Mn_{3+x}Al_{1-x}C$ with low Al content. The evidence of the unstable structure of low Al content $Mn_{3+x}Al_{1-x}C$ can also be found in the Al-free Mn_4C, which had been proved to be unstable at room temperature [7]. The presence of trace amount of carbon in $Mn_{2.75}Al_{1.25}C$ and Mn_3AlC, and the existence of a small amount of α-Mn were ascribed to the inhomogeneity of the samples during melting and casting processes.

The XRD patterns of the 1273 K homogenized

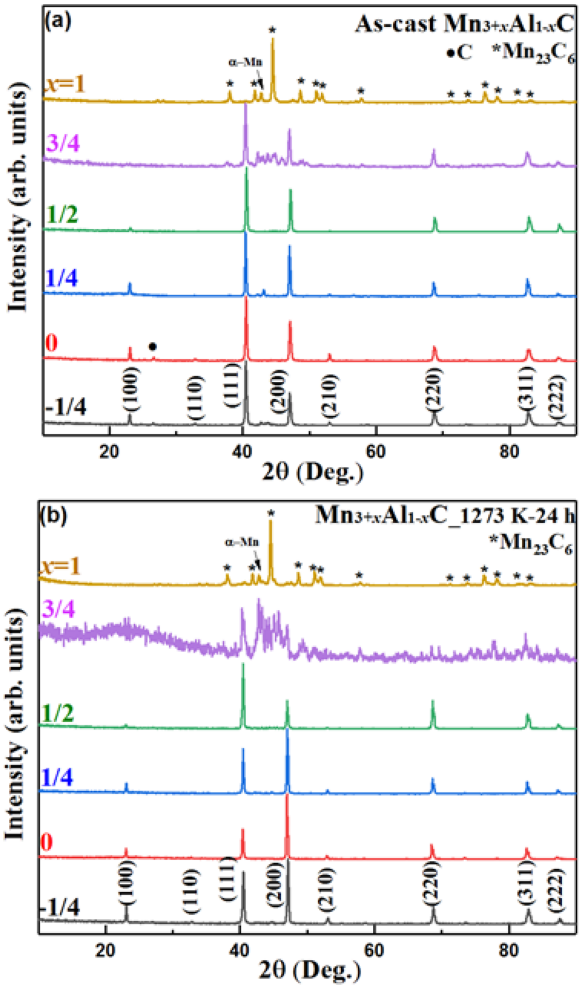

Fig. 2. (Color online) The X-ray diffraction patterns of (a) the as-cast and (b) the 1273 K homogenized $Mn_{3+x}Al_{1-x}C$ alloys with x = −1/4, 0, 1/4, 1/2, 3/4, and 1.

$Mn_{3+x}Al_{1-x}C$ (x = −1/4, 0, 1/4, 1/2) alloys could be indexed with the cubic perovskite-type structure, as shown in Fig. 2(b). For a fixed carbon content of 20 at.% in $Mn_{3+x}Al_{1-x}C$, the formation of the single phase over the composition range of Mn 55-70 at.%+Al 25-10 at.% indicates that Mn might occupy the cube corner positions while the Al atoms might occupy face center positions also. Very little change in lattice parameter was found for considerable variation in Mn/Al ratio which implies that the Mn and Al atoms have similar atomic size in these alloys. However, a further increase of Mn concentration to 75 at.%+Al 5 at.% resulted in the decreasing of the phase with cubic perovskite-type structure and the increasing of the secondary phase of $Mn_{23}C_6$ in the $Mn_{3.75}Al_{0.25}C$ samples, indicating enhanced decomposition of the unstable $Mn_{3.75}Al_{0.25}C$ during high temperature homogenization. Very weak diffraction peaks of manganese and carbon also appear in the $Mn_{3.75}Al_{0.25}C$ samples after homogenization.

It is interesting that the intensity of the (111) peak is higher than that of the (200) peak of the as-cast $Mn_{3+x}Al_{1-x}C$ (x = –1/4, 0, 1/4), whereas the relative intensities of (111) and (200) peaks reversed after high temperature homogenization, as shown in Fig. 2(a). and (b). The enhanced intensity of (200) peak of $Mn_{3+x}Al_{1-x}C$ (x = –1/4, 0, 1/4) after homogenization was ascribed to the reordering of the inhomogeneous Mn and Al atoms in the lattices through high temperature diffusion process. The atomic displacement may occur when high temperature melts were casted at a high cooling rate into bulk alloys. The structure of the $Mn_{3+x}Al_{1-x}C$ is more stable for the Mn atoms to occupy the face centered sites in the lattice. The homogenization process may enhance the occupation of Mn atoms at the face centered sites. As a result, the (200) diffraction peak would be enhanced when more Mn atoms diffuse into the face centered sites for the sum of the atomic scattering factors of Mn and C atoms is larger than that of the Al atoms. The occurrence of the intensity reversal between (111) and (200) peaks is further evidence for the mixed occupations of the Mn/Al atoms at the corner and face center positions of the lattices. It also indicates that Mn atoms are easier to occupy the face-centered position than cube corner position.

Figure 3 shows the temperature dependence of the normalized magnetizations of the samples. The Curie temperature (T_c), determined from the maximum of dM/dT, of the homogenized Mn_3AlC is measured to be 309 K, which is slightly higher than that reported by Zhang et al. but lower than that reported by Tong *et al.* [6, 9] It seems the T_c of Mn_3AlC is sensitive to the preparation conditions for which might influence the amount of the manganese loss, the defects in the lattices, and the homogeneity of the final products, and this has to some extent been proved by the variation of the T_c between the as-cast and the homogenized Mn_3AlC in our work.

Figure 3 shows that the T_c of the as-cast Mn_3AlC is slightly higher than that of the homogenized Mn_3AlC. Moreover, the gradient of the M-T curves near T_c of the as-cast Mn_3AlC is slightly lower than that of the homogenized Mn_3AlC. In addition, the M of the homogenized Mn_3AlC approaches to zero in a broader temperature range than that of the as-cast Mn_3AlC does. We speculate that the smaller dM/dT at T_c and the broader temperature region for M to approach zero in the homogenized Mn_3AlC might be ascribed to the precipitation of impurities during homogenization, which was confirmed by the additional two weak diffraction peaks at $2\theta = 70°$-$80°$ in the homogenized Mn_3AlC, as seen in Fig. 2. The earlier studies on Mn_3AlC reported the Curie temperature with different values from 290 to 310 K [10, 11]. The T_c of the homogenized $Mn_{3.25}Al_{0.75}C$, $Mn_{3.5}Al_{0.5}C$, and $Mn_{3.75}Al_{0.25}C$ alloys is determined by dM/dT to be 603, 816, and 880 K, respectively. It is interesting that the T_c of $Mn_{3+x}Al_{1-x}C$ in the range of $1 \geq x \geq 0$ increase with increasing Mn content, indicating enhanced exchange coupling of Mn atoms with increasing Mn content. The T_c of the $Mn_{3.75}Al_{0.25}C$ alloys is quite close to that of the pure Mn_4C phase we recently obtained [8]. The T_c of Mn_3AlC_y ($1.4 \geq y \geq 1$) was reported to be lower than 364 K [8]. For comparison, the Mn/Al ratio has a much greater influence on the T_c of $Mn_{3+x}Al_{1-x}C_y$ than carbon concentration has. The broad temperature region for magnetic transition of $Mn_{3.75}Al_{0.25}C$ alloys near its T_c was ascribed to the unstable structure of the magnetic phase at elevated temperatures.

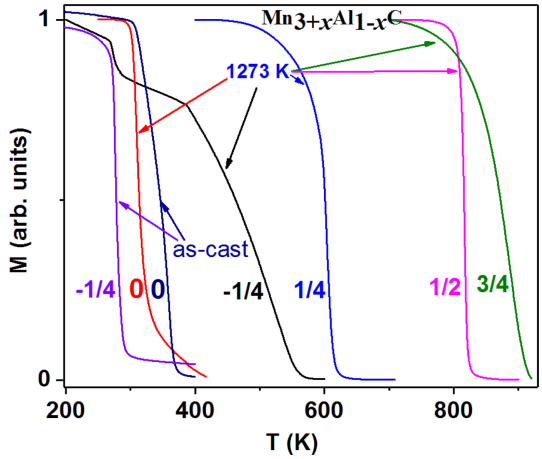

Fig. 3. (Color online) The normalized M-T plots of the as-cast $Mn_{3+x}Al_{1-x}C$ (x = –1/4, 0) and the 1273 K homogenized $Mn_{3+x}Al_{1-x}C$ (x = –1/4, 0, 1/4, 1/2 and 3/4).

The T_c of the Mn_3AlC decreases while the T_c of the $Mn_{2.75}Al_{1.25}C$ increases after annealing the as-cast alloys at 1273 K for 24 hours. The T_c of the as-cast $Mn_{2.75}Al_{1.25}C$ alloys is determined to be 276 K, which is lower than that of the Mn_3AlC alloys. However, the 1273 K homogenized $Mn_{2.75}Al_{1.25}C$ alloys exhibit two magnetic transition temperature regions, i.e. ~276 K and ~390-560 K, even though the XRD patterns of the samples imply a single phase. The large separation of T_c in the homogenized $Mn_{2.75}Al_{1.25}C$ alloys may be ascribed to the incomplete reordering of the Mn and Al atoms in the lattices at high temperatures. As mentioned above, the as-cast $Mn_{2.75}Al_{1.25}C$ may exhibit larger mutual-substitution of Mn and Al atoms for high cooling rate. The randomly occupied Mn and Al atoms may reorder to form a thermally more state when homogenized at 1273 K. The (111) reflection peak shows a stronger intensity than that of the (200) peak in the as-cast $Mn_{2.75}Al_{1.25}C$ whereas a reversed intensities of (111) and (200) peaks were observed in the homogenized

$Mn_{2.75}Al_{1.25}C$, as shown in Fig. 2. The (200) plane tends to be occupied by Mn atoms whereas the (111) plane tends to be occupied by Al atoms, as seen in Fig. 1. It is known that different atoms have different atomic diffraction factor. The intensity reversal between (111) and (200) lines in the XRD patterns of the as-cast and the homogenized $Mn_{2.75}Al_{1.25}C$ proved that reordering of Mn and Al atoms occurred. The ferromagnetism of Mn atoms was usually controlled by the degree of atomic separation.

Figure 4 shows the M-H curves of the as-cast and homogenized $Mn_{3+x}Al_{1-x}C$ samples measured at 100 K in an applied field up to 3 T. Most samples with varied x exhibit zero coercivity and zero remanent magnetization, indicating soft ferromagnetic behaviors of these alloys, in agreement with the previous reports [6, 10, 11]. The saturation magnetization (M_s) of the as-cast Mn_3AlC reaches up to 91.82 Am^2/kg, which is the largest value among that of all the samples with different compositions. The magnetic moment of Mn in the as-cast Mn_3AlC is thus estimated to be 1.00 μ_B per Mn atom. The M_s of the as-cast $Mn_{3.25}Al_{0.75}C$ alloys is 62.05 Am^2/kg, corresponding to 0.81 μ_B per Mn atom. The M_s of the as-cast $Mn_{3.5}Al_{0.5}C$ alloys is 45.28 Am^2/kg, corresponding to 0.77 μ_B per Mn atom. It should be noted that excess Mn atoms that occupying the Al sites usually magnetically coupled antiparallel to the face center Mn atoms, thus the average magnetic moment of Mn atoms is reduced with increasing Mn. The M_s of the as-cast $Mn_{3.75}Al_{0.25}C$ alloys is significantly reduced to 11.36 Am^2/kg, owing to the appearance of the non-magnetic phase and the antiparallel coupling of the excess Mn atoms to the face center Mn atoms in the residual magnetic phase. The M_s of the as-cast $Mn_{2.75}Al_{1.25}C$ alloys is slightly reduced compared to that of the as-cast Mn_3AlC alloys, owing to the reduction of the total Mn atoms.

The M_s of the homogenized $Mn_{3+x}Al_{1-x}C$ samples is lower than that of the corresponding as-cast $Mn_{3+x}Al_{1-x}C$

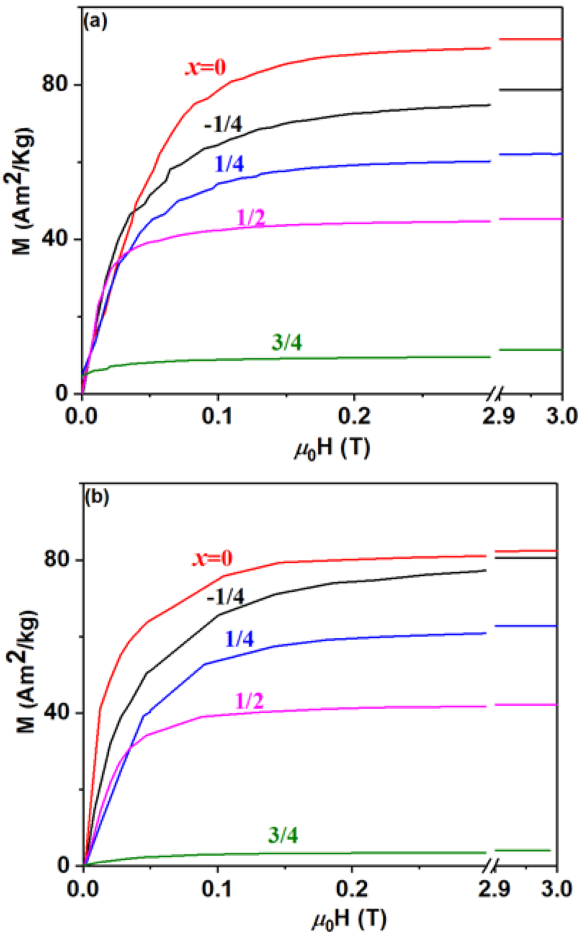

Fig. 4. (Color online) The M-H curves of the as-cast (a) and homogenized (b) $Mn_{3+x}Al_{1-x}C$ (x = −1/4, 0, 1/4, 1/2 and 3/4) measured at 100 K with field up to 3T.

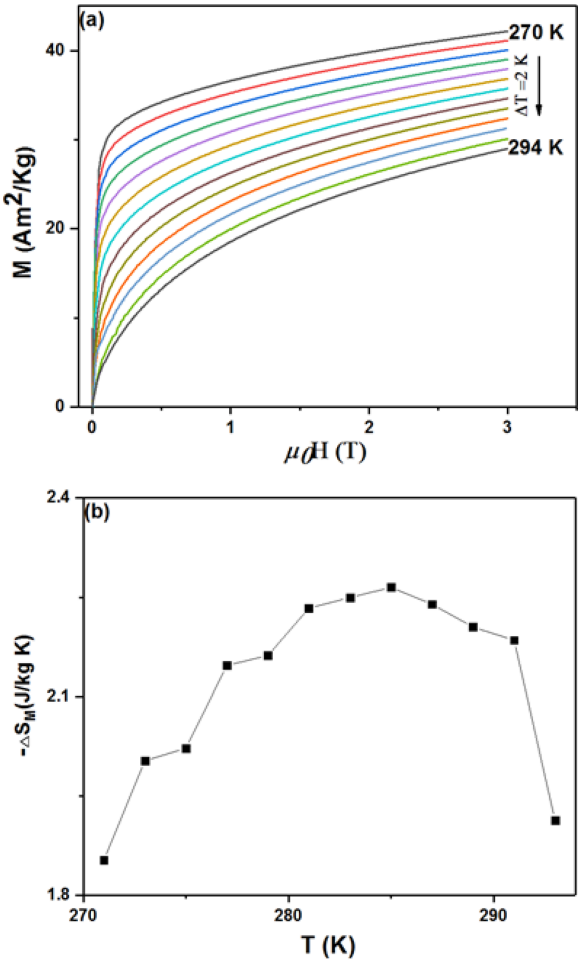

Fig. 5. (Color online) (a) Isotherm magnetization curves for $Mn_{2.75}Al_{1.25}C$ in the temperature range of 270-294 K with external magnetic fields up to 3 T. (b) Magnetic entropy change $-\Delta S_M$ as a function of temperature with external magnetic field up to 3 T for $Mn_{2.75}Al_{1.25}C$.

samples. The number of Mn atoms increases at the cube corner for $Mn_{3+x}Al_{1-x}C$ samples with varied x after homogenization, which leads to a magnetic moment reduction of Mn atoms. It can be reflected by the intensity reversal between (111) and (200) lines from the XRD patterns. So the M_s of the $Mn_{3+x}Al_{1-x}C$ samples decreases after homogenization at elevated temperatures. For the $Mn_{3.75}Al_{0.25}C$ alloys, the M_s decreasing is mainly caused by the partial decomposition of magnetic phase. The stability of the $Mn_{3.75}Al_{0.25}C$ alloys is similar to that of the Mn_4C, which is metastable and tends to decompose at high temperatures.

Figure 5(a) presents the initial isothermal magnetization curves of the as-cast $Mn_{2.75}Al_{1.25}C$ in temperature range from 270 K to 294 K at the interval of 2 K. The as-cast $Mn_{2.75}Al_{1.25}C$ sample was cooled down from 300 K under zero magnetic field to the temperature where the M(H) curve was measured. All the curves are reversible during the increasing/decreasing field cycles without any hysteresis. The behavior of non-hysteresis is helpful for practical applications of this material in magnetic refrigeration.

According to the classical thermodynamical theory and Maxwell's relation, $-\Delta S_M(T, H)$ induced by the variation in a magnetic field from 0 to H is given by [4, 5, 12, 13]

$$\Delta S_M(T, H) = S_M(T, H) - S_M(T, 0) = \int_0^H \left(\frac{\partial M}{\partial T}\right)_H dH \quad (1)$$

For the magnetization measured at small discrete field and temperature intervals, $-\Delta S_M$ can be approximately expressed by [4, 5, 12, 13]

$$\left|\Delta S_M\left(\frac{T_i + T_{i+1}}{2}\right)\right| = \Sigma\left[\frac{(M_i - M_{i+1})_{H_i}}{T_{i+1} - T_i}\right]\Delta H_i \quad (2)$$

where M_i and M_{i+1} represent the experimental values of the magnetizations at T_i and T_{i+1} under the same magnetic fields, respectively. From Eq. (2), $-\Delta S_M$ associated with the magnetic field and/or temperature variation has been calculated from the measured *M-H* curves shown in Fig. 5(a). As shown in Fig. 5(b), the maximum value of $-\Delta S_M$ is about 2.26 J/kg K for $Mn_{2.75}Al_{1.25}C$ at ~285 K under the magnetic field up to 3 T. The result is similar to the maximum value of $-\Delta S_M$ of ~2.35 J/kg K for Mn_3AlC under the same magnetic field reported by Wang *et al.* [5].

4. Conclusions

The $Mn_{3+x}Al_{1-x}C$ alloys (x = –1/4, 0, 1/4, 1/2, 3/4, and 1) were prepared by induction melting and subsequent annealing at 1273 K for 24 hours. Single phase with cubic perovskite-type structure was obtained in $Mn_{3+x}Al_{1-x}C$ with x = –1/4, 0, 1/4, and 1/2. However, a considerable amount of impurities was detected when $x = 3/4$ while $Mn_{23}C_6$ was formed when $x = 1$. The Curie temperature (T_c) of homogenized Mn_3AlC was measured to be 309 K. The magnetic moment per Mn atom decreases and the Tc increases with increasing Mn:Al ratio. The T_c of $Mn_{3+x}Al_{1-x}C$ alloys with varied x changes slightly after annealing. Most samples with varied x exhibit zero coercivity and zero remanent magnetization, indicating soft ferromagnetic behaviors of these alloys. The maximum value of the magnetic entropy changes of $Mn_{2.75}Al_{1.25}C$ is about 2.26 J/kg K at 285 K and fields up to 3 T.

Acknowledgments

We thank the National Natural Science Foundation of China (Nos. 51671177, 11074227), and the financial support from the Future Materials Discovery Program through the National Research Foundation of Korea (NRF) funded by the Ministry of Science, ICT, and Future Planning (2016M3D1A1027835).

References

[1] R. G. Butters and H. P. Myers, The London, Edinburgh, and Dublin Philosophical Magazine and Journal of Science **46**, 895 (1955).
[2] Y. Medkour, A. Roumili, D. Maouche, A. Saoudi, and L. Louail, J. Alloy. Compd. **541**, 75 (2012).
[3] Y. C. Wen, C. Wang, Y. Sun, G. X. Liu, M. Nie, and L. H. Chu, J. Alloy. Compd. **489**, 289 (2010).
[4] B. S. Wang, C. C. Li, S. Lin, J. C. Lin, L. J. Li, P. Tong, W. J. Lu, X. B. Zhu, Z. R. Yang, W. H. Song, J. M. Dai, and Y. P. Sun, J. Magn. Magn. Mater. **323**, 2017 (2011).
[5] B. S. Wang, J. C. Li, P. Tong, L. Zhang, W. J. Lu, X. B. Zhu, Z. R. Yang, W. H. Song, J. M. Dai, and Y. P. Sun, J. Appl. Phys. **108**, 093925 (2010).
[6] P. Tong, Y. P. Sun, B. C. Zhao, X. B. Zhu, and W. H. Song, Solid State Commun. **138**, 64 (2006).
[7] H. Shimizu, K. Terao, K. Motizuki, and N. Suzuki, J. Fac. Sci. **30**, 25 (1995).
[8] P. Z. Si, D. Q. Hui, H. L. Ge, J. Park, and C. J. Choi, Appl. Phys. Lett. **112**, 192407 (2018).
[9] L. Zhang, B. S. Wang, Y. P. Sun, P. Tong, J. Y. Fan, C. J. Zhang, L. Pi, and Y. H. Zhang, Phys. Rev. B **85**, 104419 (2012).
[10] F. Grandjean and A. Gérard, J. Phys. F: Met. Phys. **6**, 451 (1976).
[11] A. Kenmotsu, T. Shinohara, and H. Watanabe, J. Phys. Soc. Jpn. **32**, 377 (1972).
[12] M. H. Phan and S. C. Yu, J. Magn. Magn. Mater. **308**, 325 (2007).
[13] K. A. Gschneidner, Jr. and V. K. Pecharsky, Annu. Rev. Mater. Sci. **30**, 387 (2000).